Turk Neurosurg, 2023

Original Investigation

DOI: 10.5137/1019-5149.JTN.41242-22.2

Received: 21.01.2023
Accepted: 23.01.2023

Published Online: 06.06.2023

Endoscopic Anatomical Study of the Glabellar Keyhole Approach

Hao WU[1,2], Chenxu KONG[2], Zhengcun YAN[2], XiaoDong WANG[2], Xingdong WANG[2], Min WEI[1,2], Hengzhu ZHANG[2]

[1]Graduate School of Dalian Medical University, 9 Western Section, Lvshun South Street, Lvshunkou District, Dalian, P.R.China
[2] Yangzhou University, Clinical Medical College, Department of Neurosurgery, 225001, 98 Nantong Xi Lu, Yangzhou, Jiangsu Province, P.R.China

Corresponding author: Hengzhu ZHANG ✉ zhanghengzhu@sina.com

ABSTRACT

AIM: This study aimed to observe the exposure range of a neuroendoscope through the glabellar approach and measure the anatomical parameters to provide a basis for clinical application.

MATERIAL and METHODS: A total of 10 adult cadaveric heads fixed with formalin were dissected by stratified local anatomy and simulated operation. The length of each point was measured from the corresponding anatomical mark of the anterior fossa on the bone window plate and analysed to clarify relevant surgical indications and feasibility to provide an anatomical basis for clinical application.

RESULTS: The distance from the lower boundary of the bone window to the left anterior clinoid process was (61.97 ± 3.51) mm, the distance to the right anterior clinoid process was (62.21 ± 3.20) mm, the distance to the leading edge of the optic chiasma was (67.40 ± 5.38) mm, the distance to the sellar tubercle was (57.91 ± 2.64) mm, the distance to the centre of the saddle septum was (68.45 ± 4.88) mm; the distance to the midpoint of the endplate was (67.86 ± 4.91) mm, the distance to the anterior communicating artery was (60.89 ± 6.17) mm, the distance to the left posterior clinoid process was (67.56 ± 3.84) mm, the distance to the right posterior clinoid process was (66.78 ± 3.23) mm, the distance to the bifurcation of the left internal carotid artery was (69.45 ± 2.34) mm and the distance to the bifurcation of the right internal carotid artery was (68.01 ± 3.53) mm

CONCLUSION: The neuroendoscopic glabellar approach can effectively expose the anatomical structures of the midline anterior skull base and both sides near the sellar area and can be used to look for lesions in the midline anterior skull base.

KEYWORDS: Anatomy, Endoscopy, Glabellar approach, Keyhole, Microsurgery, Surgical approach

ABBREVIATIONS: ACA: Anterior cerebellar artery, **MCA:** Middle cerebellar artery, **ACoA:** Anterior communicating artery, **AICA:** Anterior inferior cerebellar artery, **PICA:** Posterior inferior cerebellar artery, **ICA:** Internal carotid artery, **PCoA:** Posterior communicating artery, **SCA:** Superior cerebellar artery

INTRODUCTION

In the keyhole technology, the glabella keyhole approach was proposed as the 1990s by Jho (1,6,7), an American professor of skull base neurosurgery. It is used in clinical surgery. According to their research, this approach can directly reach the anterior sellar, suprasellar, and adjacent areas through the midline of the skull base. This surgical approach was introduced in China in the early 20th century and is now used in clinical practice. Olfactory groove meningiomas and

Hao WU : 0000-0002-0858-8430
Chenxu KONG : 0000-0001-6249-6679
Zhengcun YAN : 0000-0002-3550-292X
XiaoDong WANG : 0000-0001-7233-5609
Xingdong WANG : 0000-0001-5808-7665
Min WEI : 0000-0002-3131-0955
Hengzhu ZHANG : 0000-0003-3240-5689

anterior communicating aneurysms have been successfully treated using this approach and have achieved practical clinical results (2-4). After decades of development and effort, the concept of minimally invasive neurosurgery has become popular. Minimally invasive technology has been widely used in various neurosurgical procedures, including the surgery of almost all brain lesions. Neuroendoscopy combined with the keyhole approach has emerged as one of the fastest-developing subdirections. The equipment required for neuroendoscopy is rapidly upgraded, and the application of a pneumatic arm enables surgeons to operate with both hands, completely changing the traditional mode of "one hand holding the mirror and one hand operating," and further improving the operation efficiency of neuroendoscopy (9). The neuroendoscopic combined keyhole approach is expected to further expand surgical indications while giving full play to the unique advantages of neuroendoscopy.. Therefore, this study aimed to observe the bilateral anatomical structures of the midline anterior skull base and to accomplish data measurement using a combination of neuroendoscopy and the keyhole approach (Figure 1). We believe that the results of this study can offer credible data to guide future clinical studies.

MATERIAL and METHODS

Materials

Specimens: Ten adult wet cadaveric head specimens were used. The studies were performed in the anatomy laboratory of the Clinical Medical College, Yangzhou University.

Experimental instruments: Neuroendoscope (Karl Storz, Germany [0° and 30° rigid endoscope, 4-mm diameter]), cold light source (Hangzhou Guangdian medical equipment), display screen (Sony, Japan), digital camera (Nikon COOLPIX S570 digital camera, Japan [macro 20 mm]), autopsy test bench, Vernier caliper, electric grinding drill (Medtronic), hand drill, automatic traction hook, and microscopic instruments (microscopic tweezers, scissors, and nerve retractor).

Methods

Ten adult cadaveric heads fixed with formalin were dissected using stratified local anatomy and simulated operations. The operating principle was to simulate an endoscopic glabellar surgery. A bone window of approximately 30×25 mm was made under the skin incision, and 0° and 30° endoscopes were introduced to determine a range that could be observed neuroendoscopically in the limited bone window, the operation space for neuroendoscopy, and the positional relationship between the tissue structures of the anterior fossa on endoscopy. The length of each point was measured from the corresponding anatomical mark of the anterior fossa on the bone window plate and analyzed to clarify the relevant surgical indications and feasibility to provide an anatomical basis for clinical application.

RESULTS

Skin Incision, Bone Window, and Bone Flap

Ten adult cadaveric heads were completely fixed with formalin, perfused with latex, and then kept in a supine position, slightly backward (approximately 20°–25°). A transverse horizontal incision of approximately 10 mm was made on the nasal root, and the arc was extended bilaterally to the superciliary arch. The supraorbital foramen was bounded at both ends, and an incision was made into the glabella bilaterally in an open U shape measuring approximately 4.5–5.0 cm. The nasofrontal suture was exposed inferiorly and separated superiorly into the superciliary arch. A bone window of approximately 30×25 mm was marked with a marking pen (Figure 2), and the bone flap was formed using a microgrinding drill and milling cutter. The implementation process strictly simulated the procedure of neurosurgical operation in the clinic. First, the superior sagittal sinus near the skull base was ligated, the endocranium flap was cut along the edge of the bone window, the dura was turned upward, and a part of the falx cerebri was cut. The bone crest and crista galli were removed by grinding with a micro-abrasive bur to enlarge the operating space. After dissociating the olfactory nerve, the base of frontal lobe was slightly lifted. Meanwhile, the longitudinal fissure was separated. Subsequently, 0° and 30° endoscopes were used to observe the anatomical structure at the lower limit of the endoscope at different angles. The angle of the endoscope was appropriately adjusted, the maximum range of the structures was determined bilaterally to the anterior skull base of the midline and near the sellar area, and the corresponding anatomical data were measured for analysis.

Observation and Operation of Intracranial Anatomy

Handling Method of the Superior Sagittal Sinus and Falx Cerebri

First, the superior sagittal sinus was ligated near the skull base and nasal root, and the dura mater was cut along the ring shape of the boundary of the bone window and turned superiorly. The falx cerebri was partially removed, the operation space was increased, and the height of the falx cerebri was measured. No large blood vessels were observed in the frontal pole (Figure 2).

Anterior Skull Base Bone Crest and Crista Galli

The bone crest could be observed at the lower edge of the bone window. The length and width of the bone crest in the bone window were measured, and the bone crest and crista galli were ground using a microgrinding drill. When necessary, the operative space was enlarged by grinding the medial frontal plate.

Exposure of the Operation Space to an Endoscope

The longitudinal fissure was gradually separated using micro-scissors, and the base of the bilateral frontal lobe was gently lifted with the brain spatula. The above procedure was performed sufficiently gently to not injure them. When a 0° endoscope was introduced, the first observed microscopic nerve structure was the bilateral olfactory bulb, which ran through the olfactory sulcus in the lateral and posterior parts of the crista galli. The olfactory nerve was dissociated to enlarge the perioperative visual field . The bilateral olfactory tracts were dissociated and approximated the base of the frontal lobe (Figure 2B).

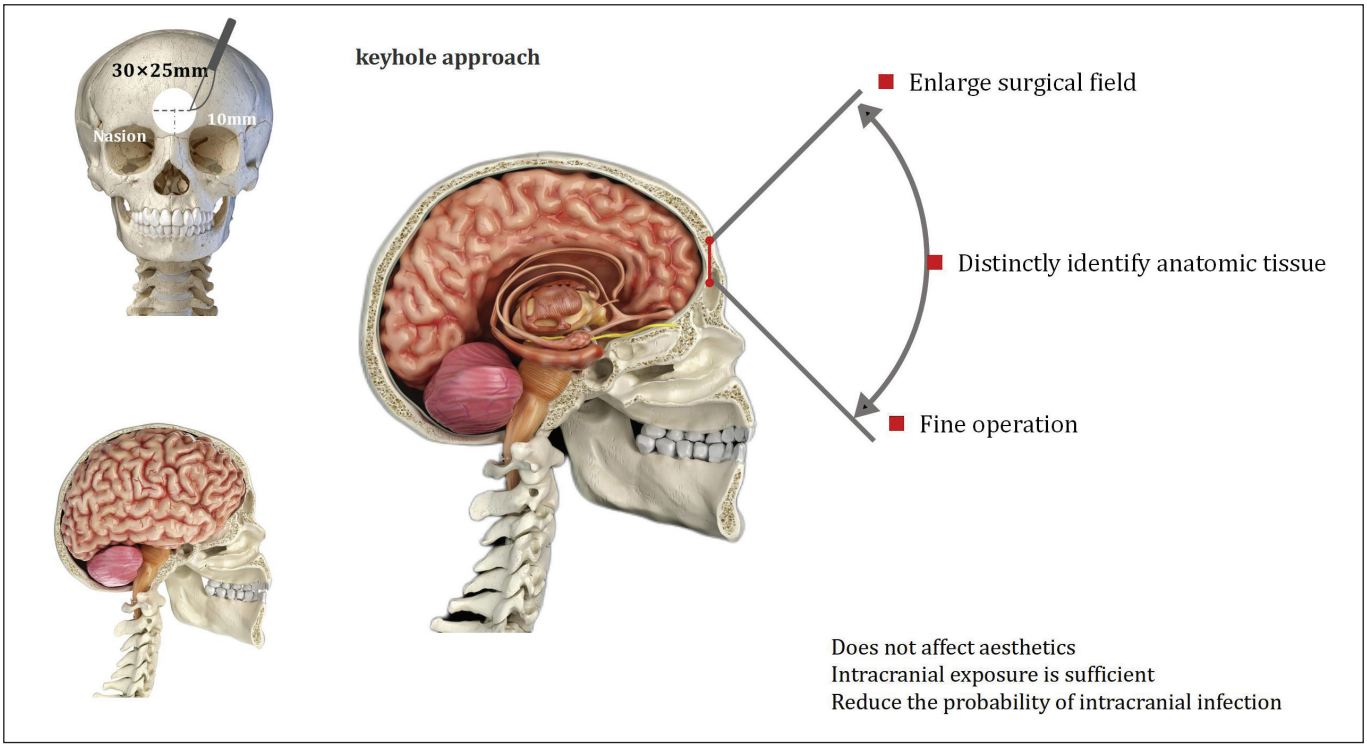

Figure 1: Keyhole approach.

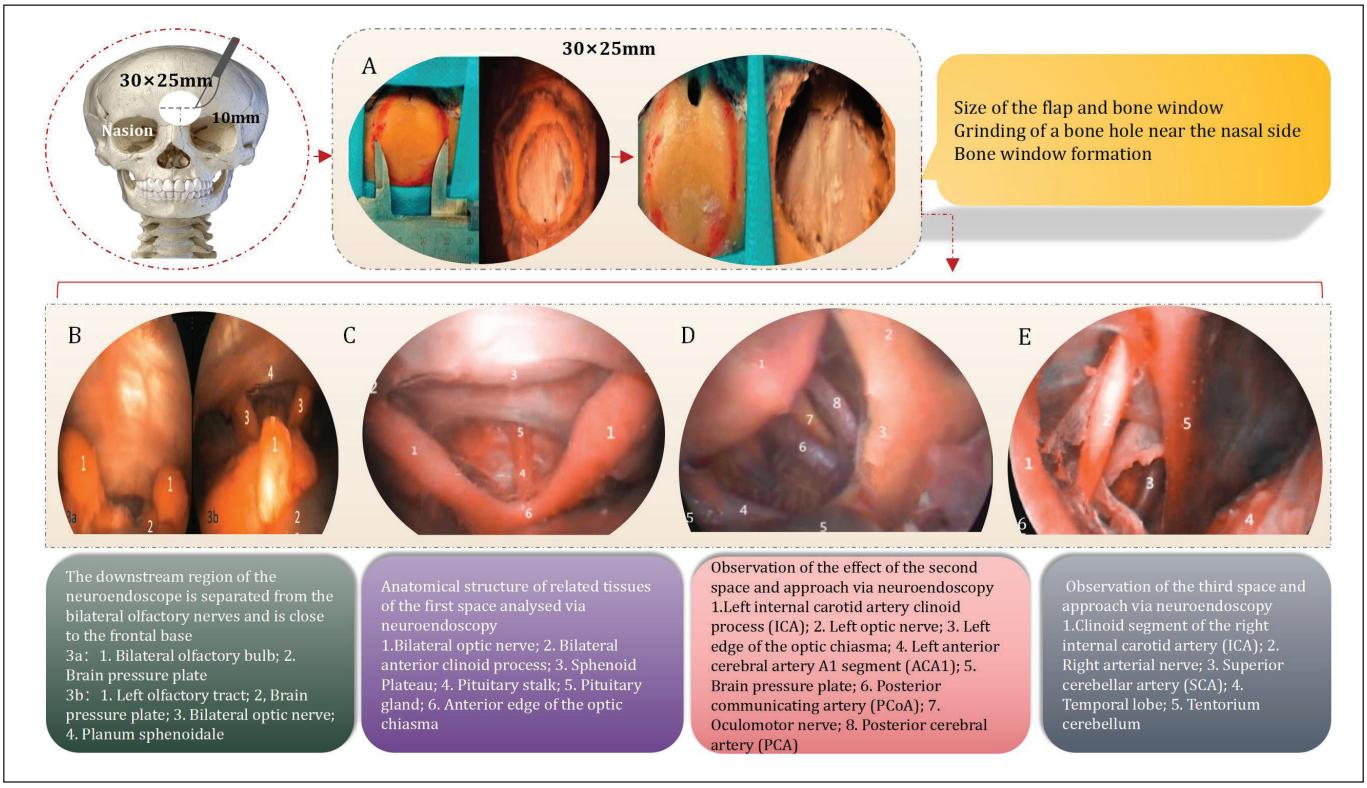

Figure 2: Anatomical tissue under endoscopy.

Specific Operation Procedures in the Cranial Cavity Using a Neuroendoscope

Exposure of the Base of the Frontal Lobe

The front and back of the bone window were observed using an endoscope. Before entering the first space, the intracranial anatomical structure can be observed, including the lamina cribrosa, crista galli, olfactory sulcus, and olfactory tract. When the neuroendoscope gradually probed the deep part of the brain, the planum sphenoidale, tuberculum sellae, and bilateral anterior clinoid processes were clearly observed.

Exposure of Each Anatomical Space of the Anterior Skull Base

Utilizing the first space, the pituitary stalk, pituitary artery, and superior pituitary artery surrounded by the bilateral optic nerve and planum sphenoidale were observed (Figure 2C). The posterior communication artery is concomitant with the oculomotor nerve, which was seen in the second space and was also the reason for the ipsilateral oculomotor nerve paralysis of the posterior communicating aneurysm. The anterior choroidal artery and its perforating branch were also observed in the second space (Figure 2D). In the third space, the oculomotor nerve was seen from back to front and outside, as well as on the inner side of the temporal lobe and parahippocampal gyrus (Figure 2E). Other perforating branches, such as the A1 segment of the anterior cerebral artery, anterior communicating artery complex, and Heubner recurrent artery, were seen in the fourth space on endoscopy (Figure 3F). Numerous perforating branches of the anterior choroidal artery were observed in the fifth space (Figure 3G).

Exposure of the Third Ventricle and Its Surrounding Structures

After opening the lamina terminalis, the base of the third ventricle (Figure 3H) and its related tissue structures were clearly observed via the neuroendoscope, especially when the opening of the midbrain aqueduct was sufficient (Figure 3I). Structures, such as the optic recess and infundibulum recess, were observed in front of the midbrain aqueduct (Figure 4J). The posterior commissure, pineal recess, and habenular commissure were observed below the midbrain aqueduct (Figure 4 K).

Observation After Adjusting the Angle of the Neuroendoscope

The trochlear nerve and superior cerebellar artery were further observed by bypassing the third space using a neuroendoscope (Figure 4L). Using a 30° endoscope, the shape of the trochlear nerve (Figure 4M) and the posterior cranial nerve tissues, such as the trigeminal and facial auditory nerves, could be clearly observed (Figure 4N).

Observation with a 30° Neuroendoscope

Introducing a 30° endoscope into the middle of the glabella revealed a wide panoramic field of vision, and the superior cerebellar artery (SCA) was observed in the deep part of the anterior skull base. By rotating the endoscope 30° on the axis, the medullary velum above the midbrain aqueduct was clearly observed at the top of the third ventricle (Figure 4O). The bilateral choroid plexus and medial thalamus were also observed.

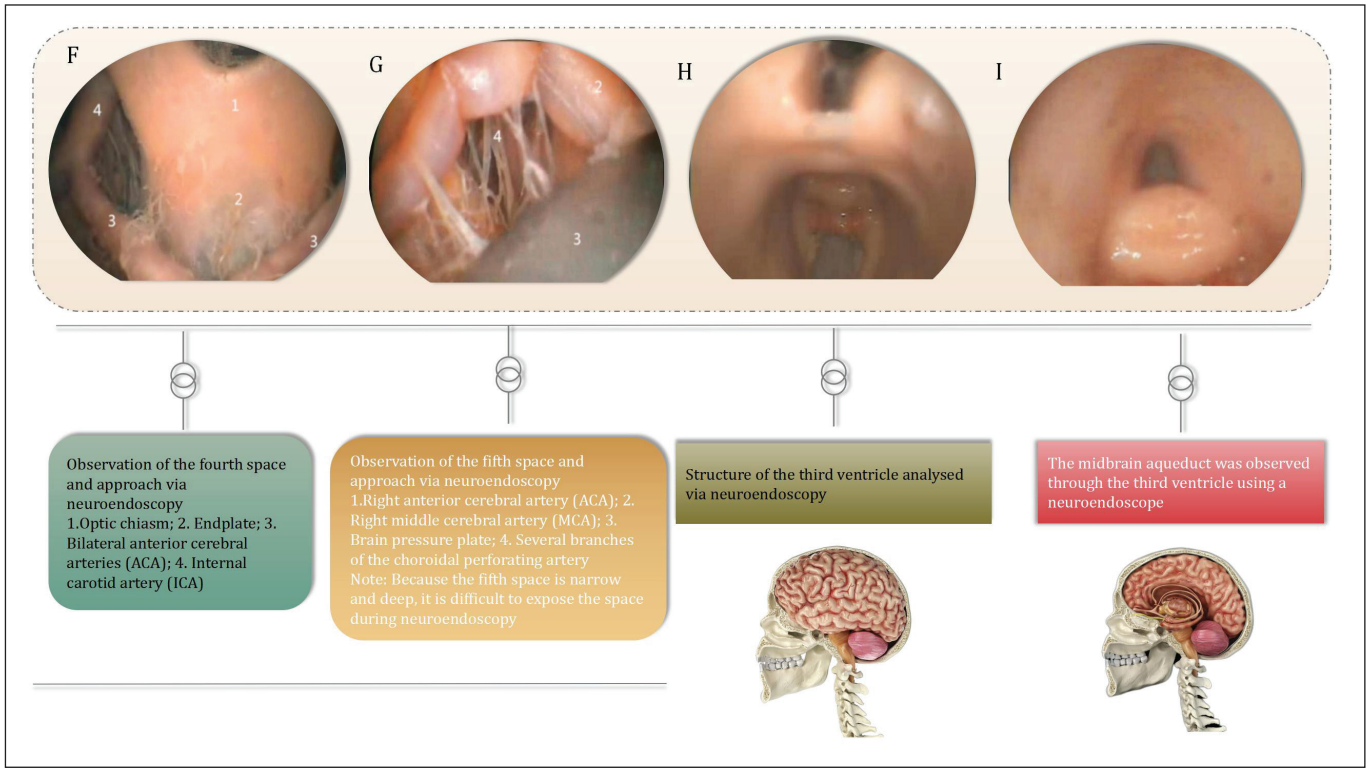

Figure 3: Anatomical details.

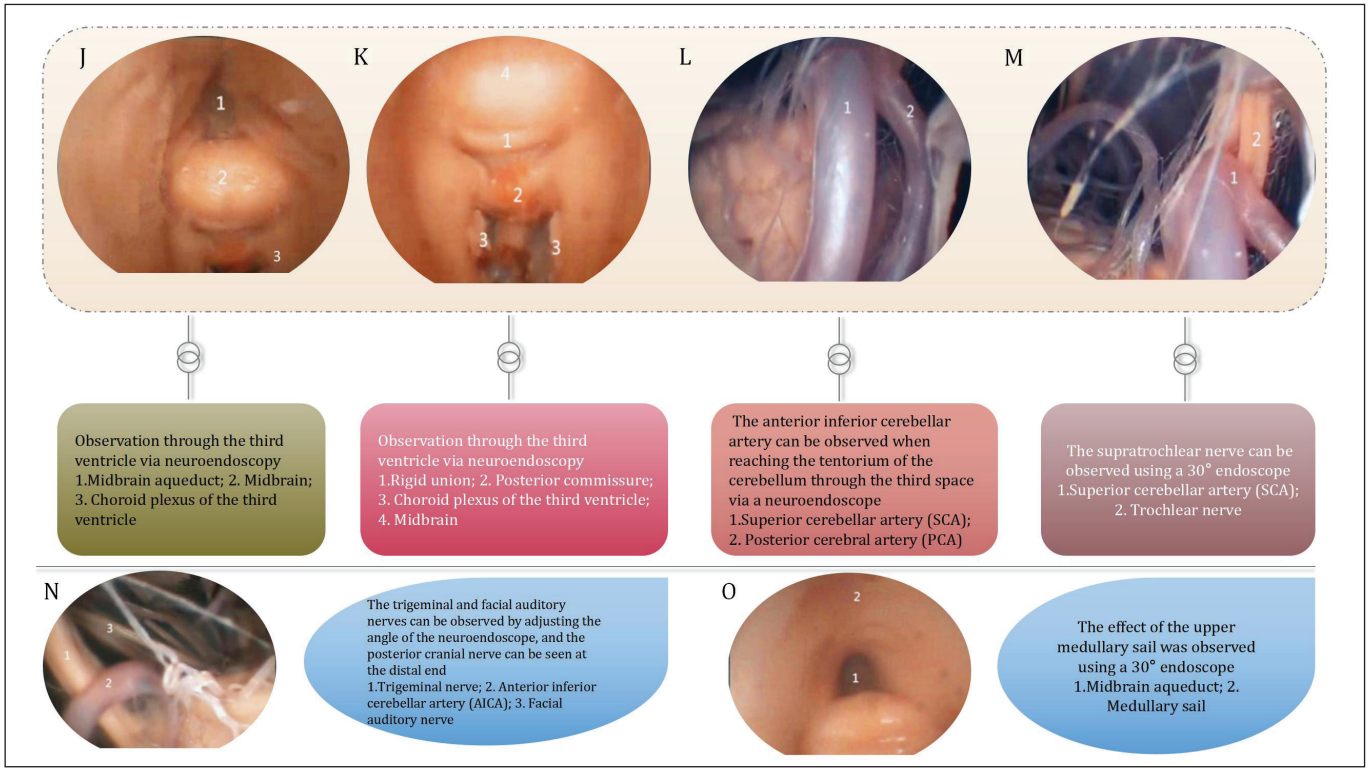

Figure 4: Third ventricle and blood vessel.

Measuring Results

A neuroendoscope was introduced into the bone window to observe the anatomical structures on endoscopy and measure the relevant data. The anatomical markers with positioning significance included the planum sphenoidale, tuberculum sellae, bilateral anterior clinoid process, and bilateral posterior clinoid process. After entering the first space, the anatomical markers included the diaphragma sellae, pituitary stalk, and pituitary gland. Optic chiasm, anterior communicating artery, and lamina terminalis were also observed. The internal carotid, anterior cerebral, and middle cerebral arteries were observed bilaterally. Opening of the lamina terminalis completely exposes the tissue structure around the third ventricle. Endoscopy provided sufficient exposure of the neurovascular structures on both sides of the midline anterior skull base. Measurement results: The distance from the lower boundary of the bone window to the left anterior clinoid process was 61.97 ± 3.51 mm, the distance to the right anterior clinoid process was 62.21 ± 3.20 mm, the distance to the leading edge of the optic chiasma was 67.40 ± 5.38 mm, the distance to the tuberculum sellae was 57.91 ± 2.64 mm, the distance to the center of the diaphragma sellae was 68.45 ± 4.88 mm; the distance to the midpoint of the lamina terminalis was 67.86 ± 4.91 mm, the distance to the anterior communicating artery was 60.89 ± 6.17 mm, the distance to the left posterior clinoid process was 67.56 ± 3.84 mm, the distance to the right posterior clinoid process was 66.78 ± 3.23 mm, the distance to the bifurcation of the left internal carotid artery was 69.45 ± 2.34 mm, and the distance to the bifurcation of the right internal carotid artery was 68.01 ± 3.53 mm (Table I).

Statistical Analysis

All data were analyzed using SPSS 17.0, and the data were expressed as mean ± standard deviation. Paired t-tests were used for statistical analysis between the means of the two groups. $P<0.05$ indicated that there was a statistically significant difference, while $p>0.05$ indicated no significant difference.

DISCUSSION

Incision Location and Bone Flap Formation

Positioning of the Glabella

The glabella is the flat part between the eyebrows, which is 10 mm above the nasal frontal suture. According to anatomy, its position is roughly equivalent to that of the frontal pole.

Surgical Incision

The incision length in this approach is approximately 5 cm, which is significantly lower (11), the incision level is low, and a transverse horizontal incision is created, which is extended bilaterally, forming a “U” shape. The position of the incision across the nasal root determines the scope of intracranial exposure and angle of the anterior skull base. Placing the incision too high is not conducive to lifting of the frontal lobe, and exposure of the frontal base is difficult, which may pose severe challenges for follow-up surgery (10). Both ends of the incision can be hidden in the eyebrows, which does not affect esthetic features. Perioperatively, attention should be paid to the width and depth of the incision, traction of the flap

Table I: Distance from Each Point of Bone Window to Intracranial Anatomical Structure (mm)

Anatomical Terms	Inferior border of the bony window	Central bone window	Left bone window	Right bone window
Left anterior clinoid process	61.97 ± 3.51	63.31 ± 2.66	60.46 ± 3.64	69.24 ± 2.58
Right anterior clinoid process	62.21 ± 3.20	62.12 ± 2.88	68.51 ± 3.05	60.19 ± 4.15
Prechiasmal border	67.40 ± 5.38	64.02 ± 4.21	67.01 ± 4.31	66.59 ± 4.01
Diaphragma sellae	68.45 ± 4.88	67.01 ± 2.64	70.58 ± 2.62	72.12 ± 3.56
Tuberculum sellae	57.91 ± 2.64	56.88 ± 3.32	60.32 ± 3.33	59.69 ± 3.25
Left internal carotid artery bifurcation	69.45 ± 2.34	67.78 ± 3.34	66.02 ± 4.04	73.27 ± 2.91
Right internal carotid artery bifurcation	68.01 ± 3.5	66.22 ± 3.79	73.52 ± 5.11	66.32 ± 4.15
Anterior communicating artery	60.89 ± 6.17	60.21 ± 5.01	63.44 ± 7.19	63.35 ± 2.65
Left posterior clinoid process	67.56 ± 3.84	66.78 ± 2.54	69.91 ± 4.16	72.61 ± 3.83
Right posterior clinoid process	66.78 ± 3.23	67.12 ± 2.58	72.14 ± 5.10	68.02 ± 3.31
Endplate midpoint	67.86 ± 4.91	65.78 ± 4.21	69.54 ± 3.64	69.85 ± 3.34

should be avoided, and the supraorbital nerve, supratrochlear nerve, and accompanying blood vessels of the same name should be protected. When making a skin incision, only the skin should be cut first to protect the muscle, followed by incision of the muscle and the periosteum under the deep muscle. This method protects the function of the supraorbital and supratrochlear nerves as much as possible, and reduces the incidence of postoperative subcutaneous effusion and cerebrospinal fluid leakage (11).

Making the Bone Window

In this study, the operating range was limited to approximately 30×25 mm. The incision was small, effectively reducing ineffective exposure and providing better exposure to bilateral structures of the anterior skull base. Additionally, the frontal sinus is often exposed when entering the anterior skull base to form a bone flap. The frontal sinus was opened in all 10 skull specimens. Therefore, radiographically understanding the development of the frontal sinus preoperatively can help operators select the method for creating a free bone flap during surgery (8).

Treatment of the Anterior Skull Base Bone Ridge, Dura Mater, and Frontal Sinus

Among the 10 skull specimens, some cadaveric head specimens had developed frontal sinuses and a large distance between the inner and outer plates of the frontal bone. After grinding the bone hole, we observed the distance between the inner and outer plates of the frontal bone and separated the two sides and upper end of the bone flap using a milling cutter. After the free bone flap was formed, the bone window reached the frontal pole level. If the exposure of the frontal base is insufficient, the internal plate of the frontal bone can be properly expanded and grounded to increase the exposure range in the bone window and operation space. A prominent frontal bone ridge was observed near the medial, middle, and lower parts of the bone window, and an upper sagittal sinus groove was observed behind the bone window. The inner plate of the frontal bone generally closely adhered to the dura mater, especially near the skull base, where the dura mater was thin and reflexed. We separated the dura mater from both sides of the bone window and eventually approached the midline. The frontal sinus was exposed because of the high surgical risk. When the frontal sinus was exposed perioperatively, if the frontal sinus mucosa was not damaged, it was to be carefully protected and covered with brain cotton. If the mucosa was damaged, it was to be washed repeatedly with iodophor and hydrogen peroxide after cleaning the damaged mucosa, and subsequently washed with mucosa, gelatin sponge, or adipose tissue. Owing to the thin frontal dura mater, especially the close adhesion between the forehead and skull base, special attention should be paid to repair the dura mater after the operation. Reverse hanging of the dura mater is a common method for preventing cerebrospinal fluid leakage. This method is feasible and can effectively reduce the incidence of postoperative cerebrospinal fluid leakage and subcutaneous effusion.

Exposure Range

Exposure to the Operation Space

The neuroendoscopic brow approach works through the midline frontal base and is combined with the longitudinal fissure approach to both sides of the midline anterior skull base and sellar region. As the falx cerebri in the bilateral frontal lobes of the longitudinal fissure can easily block the operative field, it can be partially removed to increase the field of vision. Moreover, under the falx cerebri bilateral to the frontal lobe, the bilateral gyri are often intertwined, accompanied by arachnoid adhesions; therefore, it is difficult to separate. The arachnoid on both sides should be carefully separated during the operation to increase the exposure width of the longitudinal fissure. After the neuroendoscope entered the

skull cavity, the first microscopic neuroanatomical structure was the olfactory tract. The olfactory tract is located in the olfactory sulcus of the skull base of the two frontal lobes and runs from the back to the outside, and from the front to the inside. Perioperatively, the bilateral olfactory nerves should be carefully separated and dissociated, which is conducive to lifting the frontal lobe and preventing damage to the olfactory tract. After separating the longitudinal fissure arachnoid and dissociating the frontal olfactory nerve, the neuroendoscopic operative space was exposed.

Exposure Range of the Bone Window on Neuroendoscopy

The dura mater was observed from front to back using an endoscope after opening it in the bone window. Before entering the first space, intracranial anatomical structures were observed, including the sieve plate, crista galli, olfactory sulcus, and olfactory tract. At a greater depth of the endoscope, structures such as the planum sphenoidale, tuberculum sellae, and anterior clinoid process were observed. The pituitary stalk, pituitary and superior pituitary arteries surrounded by the bilateral optic nerve and planum sphenoidale were seen through the first space. The posterior communicating artery and oculomotor nerve were seen in the second space, which is also the root of ipsilateral oculomotor nerve paralysis owing to posterior communicating artery aneurysms. The anterior choroidal artery and small perforating branches were observed in the second space. In the third space, the oculomotor nerve was seen from outside to inside, along with the inner side of the temporal lobe and parahippocampal gyrus. The cerebellar tentorium was observed in the third space. The trochlear and superior cerebellar arteries are also observed. The trochlear nerve was completely exposed using a 30 °endoscope. Other perforating branches, such as the A1 segment of the anterior cerebral artery, anterior communicating artery complex, and Heubner recurrent artery, were seen in the fourth space. Numerous perforating branches of the anterior choroidal artery are observed in the fifth space.

After opening the lamina terminalis through the fourth space, the base of the third ventricle and relevant tissue structures around the bottom of the third ventricle were visible, and the opening of the midbrain aqueduct was completely exposed. Structures such as the optic recess, infundibulum recess, and gray nodules were seen in front of the midbrain aqueduct. The habenular and posterior commissures were observed below the opening below the midbrain aqueduct. The medullary velum above the midbrain aqueduct was well observed with a 30° endoscope.

Endoscopic Brow Approach to Expand the Surgical Indications

The craniotomy scope of this approach is limited; however, according to the door opening effect of the keyhole, the surgical field of vision expands with the deepening of the surgical perspective (5,12). We believe that the operation is more suitable for resecting the skull base and some deep brain tumors, including some third-ventricle lesions. However, if the lesion is extensive, this approach is not recommended. In clinical surgical treatment, the interbrow approach is mainly used for cross-midline anterior skull base lesions, such as anterior skull base tumor, olfactory sulcus, and sphenoid platform meningiomas. Such tumors are often located at the anterior skull base across the midline, growing bilaterally to the midline; the tumor base is often located at the anterior skull base of the midline. In this approach, the basal part of the tumor can be directly exposed through the forehead base. The blood supply to the tumor can be cut off earlier during the operation, which provides good conditions for the resection of these lesions.

In addition, when combined with the longitudinal fissure approach, the interbrow approach can extend the operable space and surgical field and can directly expose the anterior cerebral artery, anterior communicating artery, and perforating branch, which is convenient for clamping aneurysms of the anterior cerebral artery, anterior communicating artery, and perforating branch. Combined with the longitudinal fissure approach, the posterior circulation artery can also be directly observed using a neuroendoscope, which can provide appropriate exposure to the vessels, including the tip of the basilar artery. Moreover, neuroendoscopy provides good results for the observation of the third ventricle and has good indications for the treatment of some third-ventricle lesions, pituitary tumors, and craniopharyngiomas growing on the saddle. Therefore, the scope of exposure through the interbrow approach via a neuroendoscope is wide, and the scope of surgical indications is wider than that of microscopy.

Therefore, the keyhole approach using a neuroendoscope is more suitable for the resection of tumors in the midline, both sides of the anterior skull base, sellar region, and deep brain. However, if the lesion range is wide and brain tissue edema is evident, making it difficult to expose the intracranial natural space, this approach is not recommended. Few clinical studies have reported on the surgical management of some posterior circulation aneurysms. In addition, the relevant clinical surgical indications warrant further investigation.

Advantages and Disadvantages of the Neuroendoscopic Keyhole Approach

Advantages

As a representative of the “keyhole” surgical technique, the advantages of the neuroendoscopic interbrow approach are evident and include the following: 1) The skin incision is located between the eyebrows, which does not affect esthetic features after healing. 2) The incision is small, the trauma of the approach was small, the intracranial exposure range was sufficient, the two sides of the anterior skull base of the midline are properly exposed, and lesions in the third ventricle are well exposed. 3) The bone window is closer to the skull base, which reduces the exposure of ineffective brain tissue and reduces contusion of brain tissue, thus making complete use of the frontal floor and longitudinal fissure space to expand the operation space for endoscopy. 4) A small bone window can reduce the probability of postoperative frontal subcutaneous effusion and secondary intracranial infection.

Disadvantages

The neuroendoscopic brow approach has the following disadvantages:

1) After undergoing neuroendoscopy through the interbrow approach, patients have different degrees of frontal sinus opening, which inevitably increases the possibility of postoperative intracranial secondary infection. Moreover, the surgical is less conducive to for change, which is unsuitable for patients with a wide range of lesions in the anterior skull base and evident brain swelling. 2) Neuroendoscopy using the glabellar keyhole approach requires the operator to be proficient in the anatomy of the anterior skull base and requires advanced surgical instruments. 3) Because the incision created using this approach is small, it is difficult to suture intraoperatively. Therefore, a preoperative examination and careful surgical planning are required.

CONCLUSION

The neuroendoscopic glabellar approach can effectively expose the anatomical structures of the midline anterior skull base and both sides near the sellar area, and can be used to observe for lesions in the midline anterior skull base. This approach can completely expose the suprachiasmatic space, which is suitable for the examination of lesions in the midline of the suprasellar region and those growing in the suprasellar region. It can be used for clipping anterior communicating aneurysms and providing appropriate exposure to the tips of the basilar and posterior circulation arteries. The neuroendoscopic brow approach offers better exposure of the third ventricle. Neuroendoscopy has the advantages of facilitating close observation, a wide field of vision, and passing through a narrow space, which can increase the accuracy of surgery.

AUTHORSHIP CONTRIBUTION

Study conception and design: HW, CK
Data collection: ZY, XDW
Analysis and interpretation of results: MW, XW
Draft manuscript preparation: HW
Critical revision of the article: HZ
All authors (HW, CK, ZY, XDW, XW, MW, HZ) reviewed the results and approved the final version of the manuscript.

REFERENCES

1. Alfieri A, Jho HD: Endoscopic endonasal approaches to the cavernous sinus: surgical approaches. Neurosurgery 49(2):354-360,2001
2. Bhattarai R, Liang C, Chen C, Wang H, Huang T, Ning X, Guo Y:Supraorbital eyebrow keyhole approach for microsurgical management of ruptured anterior communicating artery aneurysm. Exp Ther Med 20(3):2079-2089,2020
3. Bhattarai R, Liang CF, Chen C, Wang H, Huang TC, Guo Y:-Factors determining the side of approach for clipping ruptured anterior communicating artery aneurysm via supraorbital eyebrow keyhole approach. Chin J Traumatol 23(1):20-24,2020
4. Cho WS, Kim JE, Kang HS, Son YJ, Bang JS, Oh CW: Keyhole Approach and Neuroendoscopy for Cerebral Aneurysms. J Korean Neurosurg 60(3):275-281,2017
5. Hopf NJ, Perneczky: Endoscopic neurosurgery and endoscope-assisted microneurosurgery for the treatment of intracranial cysts. Neurosurgery 43(6):1330-1336,1998
6. Jho HD: Endoscopic transpedicular thoracic discectomy. Neurosurg Focus 9(4):e4,2000
7. Jho HD: Orbital roof craniotomy via an eyebrow incision: A simplified anterior skull base approach. Minim Invasive Neurosurg 40(3):91-97,1997
8. Lin Y, Qiu Y: Microanatomy of endoscope-assisted glabellar nasal keyhole approach. Minim Invasive Neurosurg 46(3):155-160, 2003
9. Nagata Y, Watanabe T, Nagatani T, Takeuchi K, Chu J, Wakabayashi T: Fully endoscopic combined transsphenoidal and supraorbital keyhole approach for parasellar lesions. J Neurosurg 128(3):685-694, 2018
10. Rychen J, Croci D, Roethlisberger M, Nossek E, Potts MB, Radovanovic I, Riina HA, Mariani L, Guzman R, Zumofen DW: Keyhole approaches for surgical treatment of intracranial aneurysms: A short review. Neurol Res 41(1):68-76, 2019
11. Sato H, Nonaka Y, Bawornvaraporn U, Fukushima T: Preauricular retromandibular trans tympanic plate and styloid process keyhole approach to parapharyngeal lesions: A laboratory study. Acta Neurochir (Wien) 162(3):661-669, 2020
12. Taniguchi M, Perneczky A: Subtemporal keyhole approach to the suprasellar and petroclival region: Microanatomic considerations and clinical application. Neurosurgery 41(3):592-601, 1997